Research Article

Deletion of the Long Non-coding RNA *ANRIL* In Addition to the Protein-Coding Genes of the INK4-ARF Locus in the A549 Cell Line: An Existing Phenomenon or a Novel Genetic Alteration?

Erfan Sherifi [ID] [1], Fardin Fathi [1], Mohammad Bagher Khadem Erfan [1], Farzad Soleimani [1], Karim Rahimi [2], Fatemeh Zamani [3], Zakaria Vahabzadeh [ID] [1, *]

[1] Cellular and Molecular Research Center, Research Institute for Health Development, Kurdistan University of Medical Sciences, Sanandaj, Iran
[2] Department of Genetics, Blavatnik Institute, Harvard Medical School, Boston, USA
[3] Lung Diseases and Allergy Research Center, Research Institute for Health Development, Kurdistan University of Medical Sciences, Sanandaj, Iran

Corresponding Author: Cellular and Molecular Research Center, Research Institute for Health Development, Kurdistan University of Medical Sciences, Sanandaj, Iran. Email: zakariav@gmail.com

Abstract

Background: A549, a human lung adenocarcinoma cell line, is a KRAS mutant cell used for over 5 decades as a type II alveolar cell and non-small cell lung adenocarcinoma model. Cyclin-dependent kinase inhibitor 2 A (*CDKN2A*) and cyclin-dependent kinase inhibitor 2 B (*CDKN2B*) are protein-coding genes in the INK4-ARF locus and function as tumor suppressors and negative regulators of the cell cycle. These genes have been reported to be deleted in the A549 cell line. The Long non-coding *RNA ANRIL* is located in the antisense direction of *CDKN2B* and shares a bidirectional promoter with *CDKN2A*. *ANRIL* is a negative regulator of the INK4-ARF locus genes and has an oncogenic role in cancers. *ANRIL* deletion in the A549 cell line has not been reported to date.

Objectives: Herein, the presence of *ANRIL* was investigated in the A549 cell line.

Methods: In this study, the A549 cell line from 2 different sources was tested for the presence of the INK4-ARF locus genes by polymerase chain reaction (PCR) using specific primers at both DNA and *RNA* levels. We compared our findings with Calu-6, MRC-5, and HepG2 cell lines.

Results: Our analysis revealed that all protein-coding genes in the INK4-ARF locus, including *CDKN2A* and *CDKN2B*, were deleted in the A549 cell lines. Furthermore, we observed that *ANRIL* was entirely deleted in the A549 cells. The evaluated locus and all of its genes are present and expressed in other investigated cell lines.

Conclusions: For the deletion of *ANRIL* in the A549 cell line, 2 scenarios are possible: First, from a structural point of view, the deletion of the protein-coding genes in the antisense of *ANRIL* in the INK4-ARF locus implies the possibility of a concurrent loss of *ANRIL* with the deletion of these genes in the A549 cell line. Second, as cancer cell lines are genetically unstable and are always susceptible to the acquisition of new mutations, *ANRIL* loss may have occurred later, following a novel genetic alte*RNA*tion in a population derived from a mutated cell.

Keywords: A549 Cell Line, *ANRIL*, INK4-ARF Locus, *P14ARF, P15INK4B, P16INK4A*

1. Background

The human lung adenocarcinoma cell line A549 was inaugurated by D.J. Giard in 1972 from grade IV lung cancer tissue removed from a 58-year-old Caucasian man and subsequently donated to the ATCC cell line bank by M. Lieber under accession number CCL-185TM (1). The A549 cell line is known as a hypotriploid alveolar basal epithelial cell. It exhibits a polarized monolayer adherent morphology and positive tannic acid staining for lamellar bodies. The production of lamellar bodies, the expression of IA1 and IIB6 P450 isoenzymes, and the endocytic abilities of these cells have made them a suitable model for use as a type II lung epithelial cell and for in vitro studies of the oxidative metabolism of drugs in the lung (2). Consistent with the pattern of

phospholipid synthesis expected for cells responsible for lung surfactant synthesis, A549 cells synthesize lecithin with a high content of unsaturated fatty acids using the cytidine diphosphocholine pathway at both early and late culture passages. Considering that A549 cells are lung adenocarcinoma-derived cells that lack tissue architecture, tumor microenvironment, and *in-situ* tumor cell communication, and retain gene expression patterns similar to tumors, it is a proper model for human lung adenocarcinoma studies (3-8).

It should be noted that Lung Adenocarcinoma, which is related to non-small cell lung carcinoma (NSCLC), is the most common type of lung cancer, accounting for about 40% of all lung cancer cases (7, 9).

Previous studies on A549 cells have shown that 24% of all A549 cells have 66 chromosomes. Most of these cells have two X and two Y chromosomes. However, in 40% of the cells examined, one or both Y chromosomes were missed (1). This cell line carries a homozygous mutation at position 12p12.1 (c.34G>A/p.Gly12Ser) of the Kirsten rat sarcoma virus (K-RAS) pro-oncogene protein (3, 10-12). Due to the homozygous deletion of the p.Gln37Ter (c.109C>T) and cyclin-dependent kinase inhibitor 2 A (*CDKN2A*) homozygous, c.1_471del471/p.M1_*157del, A549 cell line does not express the serine/threonine kinase tumor suppressor gene (*STK11*/LKB1) and *CDKN2A* locus (8, 10, 13-15). In addition, tumor suppressor in lung cancer 1 (TSLC1) and tumor suppressor *NORE1A* (*RASSF5*) are not expressed in A549 cells (16-18). However, cyclin *D*, cyclin-dependent kinases 4/6(*CDK4/6*), retinoblastoma susceptibility gene (*RB1*), transcription factor *E2F*, mouse double minute 2 homolog (*MDM2*), phosphatidylinositol-4,5-bisphosphate 3-kinase catalytic subunit alpha (*PIK3CA*), epidermal growth factor receptor (*EGFR*), tumor protein p53 (*TP53*), anaplastic lymphoma kinase (*ALK*), *MYC* proto-oncogene, and phosphatase and tensin homolog (*PTEN*) genes are expressed in the wild type as in normal cells (7, 8, 19-27).

The 9p21.3 region, spanning approximately 350 kb of the genomic region, harbors 3 protein-coding genes and a long non-coding *RNA* in the antisense direction. The protein-coding genes consisting of S-methyl-5'-thioadenosine phosphorylase (*MTAP*), *CDKN2A*, which encodes the p16^{INK4A} and *P14ARF* splice variants and cyclin-dependent kinase inhibitor 2 B (*CDKN2B*) (also known as *P15* ^{INK4B}). The long non-coding *RNA* in the antisense direction of *CDKN2B* is called *CDKN2B*-AS1/*ANRIL* (antisense non-coding *RNA* in the INK4 locus). The INK4-ARF locus, mapped to the 9p21.3 region and its gene cluster consisting of *P14ARF*, *P16* ^{INK4A}, *P15* ^{INK4B}, and long non-coding *RNA* (LncRNA) *ANRIL*. Structurally *ANRIL*

shares a bidirectional promoter with the *P14ARF* gene and transcribes *ANRIL* in antisense orientation to the INK4-ARF gene cluster. *P16* ^{INK4A} is located between *MTAP* and *ANRIL* in the vicinity of the first exon of *ANRIL*. The first exons of *P14ARF* (exon1β) and *P16* ^{INK4A} (exon1α) are different, but the second and third exons are identical. *P15* ^{INK4B} is mapped to the inside of the first intron of *ANRIL* in antisense orientation (28) (Figure 1).

When the cell is exposed to various stress signals such as DNA damage, oxidative stress, or enhancing oncogenes, the expression of INK4-ARF genes is activated. This results in a cascade of signaling events that adequately initiate the cell cycle arrest. *P14ARF*, a member of this gene cluster, interacts with the acidic domain of *MDM2* to block its interaction with P53. Nuclear segregation of *MDM2* intercepts *MDM2*-mediated delivery of P53 to the cytoplasm, thereby preventing P53 degradation. As a result, P53-dependent cell cycle arrest occurs in both G1 and G2 phases. In response to stress signals, the *P16* ^{INK4A} and *P15* ^{INK4B} are activated and attached to CDK4/CDK6 kinases. Preventing the formation of active complexes by cyclin D leads to hypo-phosphorylation of RB. Hypo-phosphorylated RB connects to the transactivation domain of E2. This complex further engages histone deacetylase 1 (HDAC1) and SUV39H1 histone lysine methyltransferase to *E2F* target genes, thereby hampering them and obstructing the G1-to-S phase transition (15, 29).

For the first time, the *ANRIL* gene was discovered through a 403 231 bp germline deletion in a French family with a history of melanoma and nervous system tumors syndrome (30). In response to genomic stress induced by DNA damage, *E2F*1 activates the transcription of *ANRIL* in an ataxia telangiectasia mutated (ATM)-dependent manner. *ANRIL* is transcribed by *RNA* polymerase II and spliced into several linear and circular isoforms in a tissue-specific manner. The complete gene has 21 exons and it has been only found in simians. Under normal circumstances, *ANRIL* binds to the SUZ12 subunit of Polycomb repressive complex 2 (PRC2) when DNA repair is complete. This binding helps to suppress the inhibitory effects of the INK4-ARF locus by inducing the methylation of histone 3 at lysine 27 (H3K27), allowing re-entry into the cell cycle; this has been suggested as a potential mechanism. In addition, *ANRIL* binds to *CBX7* of Polycomb repressive complex 1 (PRC1), enabling recognition of H3K27 for monoubiquitination of histone 2A at lysine 119 (H2AK119) to maintain silencing of the INK4-ARF locus. *ANRIL* may regulate gene transcription through
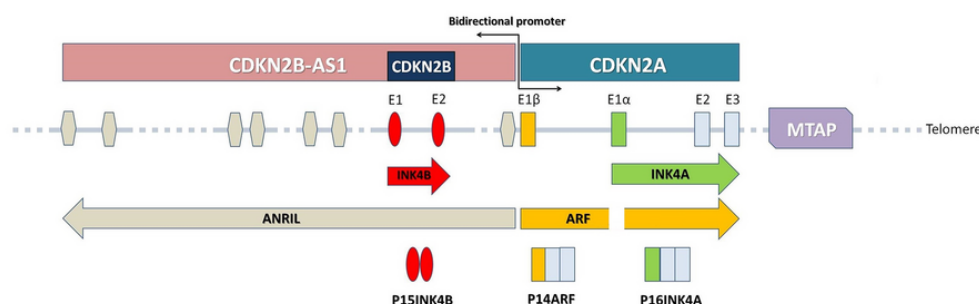
Figure 1. Schematic view of the INK4-ARF locus in the 9p21.3 chromosomal region. The INK4-ARF locus, mapped to the 9p21.3 region and consisting of the CDKN2A, CDKN2B and lncRNA *ANRIL* genes. *ANRIL* shares a bidirectional promoter with the P14ARF and transcribes *ANRIL* in antisense orientation to the CDKN2A and CDKN2B genes. P16INK4A is located between MTAP and the first exon of *ANRIL*. The first exons of P14ARF (E1β) and P16INK4A (E1α) are different, but the second and third exons are identical. CDKN2B is mapped to the inside of the first intron of *ANRIL* in antisense orientation. The A549 cell line is characterized by homozygous deletion of the CDKN2A, CDKN2B and MTAP genes.

chromatin modulation (Nuclear localization hypothesis). Circular *ANRIL* may also be involved in post-transcriptional regulation (cytoplasmic localization hypothesis) (28, 31). Recently, genome-wide association studies (GWAS) identified the *ANRIL* gene as a genetic locus commonly associated with a variety of health conditions, including intracranial aneurysm, type 2 diabetes, coronary artery disease (CAD), periodontitis (PD), Alzheimer's disease, aging, frailty, glaucoma, endometriosis, multiple sclerosis, hypertension, as well as cancer (28, 32). In cancer, *ANRIL*-micro*RNA* (mi*RNA*) interactions can influence their target genes and initiate a cascade of events that leads to the intensification of the oncogenic aspect of *ANRIL* in proliferation, metastasis, invasion, resistance to radiotherapy, drug-induced cytotoxicity and apoptosis. This occurs through the involvement of various signaling pathways such as ATM-*E2F*1, PI3K/Akt, Wnt/β-catenin, NF-κB, TGF-β/Smad, Notch, and mTOR (28, 33).

Several studies have shown a homozygous deletion of the *MTAP* (34) and protein-coding genes of the INK4-ARF locus in the A549 cell line (7, 14, 35-38); so, the deletion of the LncRNA *ANRIL* in the antisense of this region is very likely from a structural point of view (Figure 1). However, the search in the database and literature did not reveal any report regarding the lack of expression of the *ANRIL* gene in the A549 cells, and several studies have reported the expression of *ANRIL* in this cell line (39-41).

2. Objectives

The presence of the LncRNA *ANRIL* in the A549 cell line was investigated in this study.

3. Methods

3.1. Cell Lines and Cell Culture

Human NSCLC cell line A549 was purchased from 2 cell bank centers in Iran, Pasteur Institute of Iran (Tehran, Iran) and Iranian Biological Resource Center (Tehran, Iran). The validity and authenticity of the A549 cell line were guaranteed by both of the cell banks. The human NSCLC cell line Calu-6, as well as the human normal lung fibroblast cell line MRC-5 and human hepatocellular carcinoma cell line HepG2, were acquired from the Pasteur Institute of Iran's cell bank. The cell bank of the Pasteur Institute of Iran verified and authenticated these cell lines. All cells were grown in Roswell Park Memorial Institute 1640 (RPMI1640) supplemented with 10% fetal bovine serum (FBS) and 100 U/mL penicillin-streptomycin and maintained at 37°C in a humidified incubator with 5% CO_2 (Figure 2).

3.2. Genome Preparation

The adherent cells were trypsinized and collected by centrifugation at 250 g for 5 minutes. The cell pellets were, then, resuspended in phosphate buffered saline (PBS).

The DNA was isolated from the harvested cells, using the FavorPrep Tissue Genomic DNA Extraction Mini Kit (Favorgen, Taiwan), according to the manufacturer's protocol. *RNA* was extracted from collected cells, using the FavorPrep Total *RNA* Purification Mini Kit (Favorgen, Taiwan), according to the manufacturer's recommendations and 60 μL of 0.25 U/μL DNase I (Yekta Tajhiz Aama, Iran) was used during the extraction process to eliminate any possible contamination of the
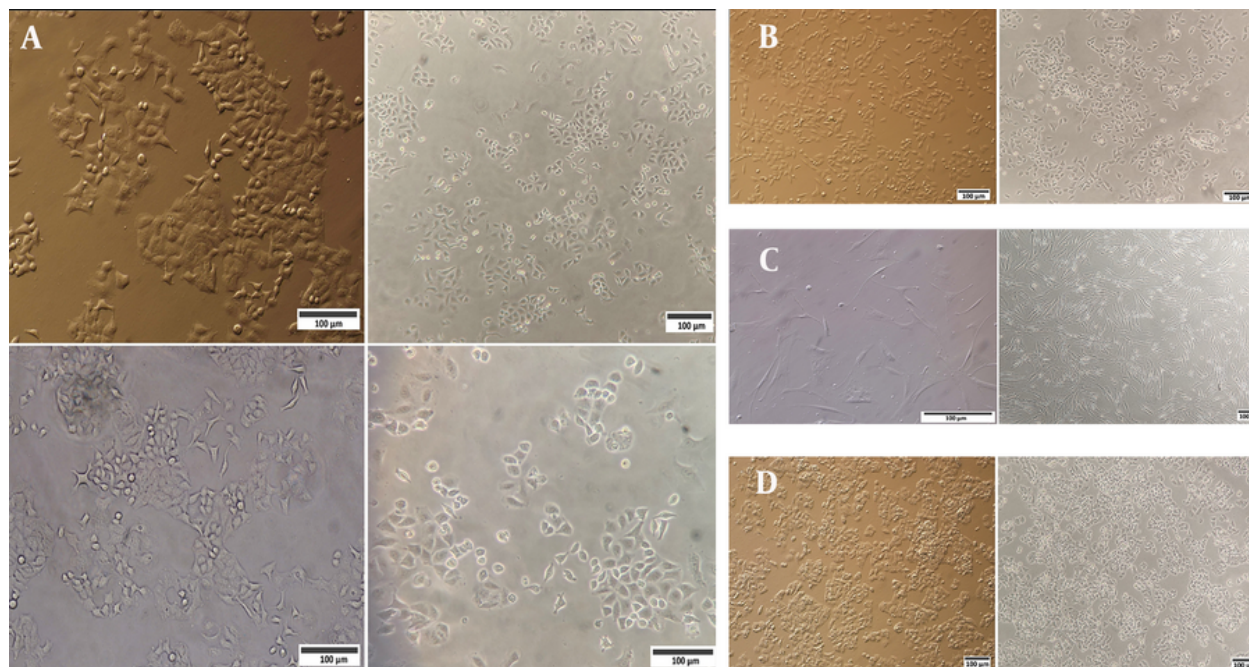
Figure 2. Cell morphology of the A, A549; B, Calu-6; C, MRC-5; and D, HepG2 cell lines. Scale bars: 100 μm.

genomic DNA. The samples were kept at -80°C until further processing. The quantity and quality of extracted DNA and *RNA* were checked, using a Nanodrop spectrophotometer (Thermo Scientific™ NanoDrop™ One, USA).

To evaluate the integrity and quality of the *RNA* and genomic DNA, we conducted an agarose gel electrophoresis, using 1% agarose and TAE running buffer.

Total *RNA* (1 μg) was reverse transcribed into cDNA, using a cDNA Synthesis Kit (catalog number: YT4500, Yekta Tajhiz Azma, Iran) containing random hexamer primers and M-MLV reverse transcriptase according to the manufacturer's instructions.

3.3. Polymerase Chain Reaction

The presence of the target sequences in obtained cDNA and genomic DNA from cell lines was checked by performing a polymerase chain reaction (PCR) reaction with specific primers (Table 1). Glucose 6-phosphate dehydrogenase (G6PD) and glyceraldehyde-3-phosphate dehydrogenase (GAPDH) genes were used as common isoenzyme markers and inte*RNA*l controls for DNA and cDNA, respectively, in all cell lines.

The PCR reaction was carried out according to the procedure of the 2X PCR master mix kit (Yekta Tajhiz Azma, Iran). The reaction mixture was as follows: Ten μL of master mix, 0.25 μL of forward and reverse primer (10 μM), 1 μL of DNA/cDNA template, and 8.5 μL nuclease-free water to a final reaction volume of 20 μL. A no-template control (NTC) was included for each primer pair.

The thermal cycle programs were as follows: Initial denaturation for 5 minutes at 94°C, followed by 40 cycles of 94°C for 20 seconds, Annealing 56 - 60°C (based on primer annealing tm) for 20 seconds, and extension at 72°C for 20 seconds. The final extension was 72°C for 5 minutes.

The PCR products were confirmed by 2% agarose gel electrophoresis, using Tris-acetate-EDTA (TAE) running buffer and visualized on a UV transilluminator.

3.4. Real-time PCR

Real-time PCR was performed to assess *ANRIL* expression in cDNA libraries from Calu-6 and A549 cell lines with the protocol of Smart Green qPCR (real-time) master mix (Yekta Tajhiz Azma, Iran) containing primers for *ANRIL*- RT1, *ANRIL*- RT2 (Table 1), using a LightCycler® 96 instrument (Roche, Germany) for 45 cycles as follows

Table 1. The List of Primers for Amplification of the Target Sequences in the INK4-ARF Locus at the 9p21 Region

Primer Name and Accession Number	Primer Sequences	Size of Product (Base Pair)	Template
P14^{ARF} (NM_058195.4)	Forward: 5'- AGTGAGGGTTTTCGTGGTTC -3'	93	DNA/cDNA
	Reverse: 5'- AGTAGCATCAGCACGAGGG -3'		
P15^{INK4B}(CDKN2B)(NM_004936.4)	Forward: 5'- TGGGAAAGAAGGGAAGAGTGTC -3'	173	DNA/cDNA
	Reverse: 5'- TCGCACCTTCTCCACTAGTC -3'		
P16^{INK4A}(CDKN2A)(NM_058197.5)	Forward: 5'- AGCAGCATGGAGCCTTCG -3'	124	DNA/cDNA
	Reverse: 5'- GCCTCCGACCGTAACTATTC -3'		
ANRIL 1 (NC_000009.12)	Forward: 5'- TCACCTGACACGGCCCTACC -3'	292	DNA
	Reverse: 5'- TCAGAGGCGTGCAGCGGTTTAG -3'		
ANRIL 2 (NC_000009.12)	Forward: 5'- ATGCTTTCTTTAGATCAACCCAG -3'	356	DNA
	Reverse: 5'- TACTCTGGCAAGACGGAGG -3'		
ANRIL 3 (NC_000009.12)	Forward: 5'- ATTGTCCATATCACTTAACCAGTTG -3'	348	DNA
	Reverse: 5'- TCATCACAGCAGTACAGAGGAAG -3'		
ANRIL 4 (NC_000009.12)	Forward: 5'- AATTGAAGGATCAGGGAGTCAG -3'	497	DNA
	Reverse: 5'-ATTCCCATGATTCACTGTAGGC -3'		
ANRIL 5 (NC_000009.12)	Forward: AAGTGGCAGGAATTTGGGAATG -3'	84	DNA
	Reverse: AGTCACTGGTCTGAGTTCTTAAA -3'		
ANRIL 6 (NC_000009.12)	Forward: 5'- TAATGCTTACCTAGTGCCAGATG -3'	165	DNA
	Reverse: 5'- AAATCCCAGCCAATTACCAGCG -3'		
ANRIL - RT1 (NR_003529)	Forward: 5'-AGAGAGGGTTCAAGCATCAC -3'	121	cDNA
	Reverse: 5'-TCTGATGGTTTCTTTGGAGTTAG -3'		
ANRIL - RT2 (NR_003529)	Forward: 5'- TTATTCCTGGCTCCCCTCGTC -3'	222	cDNA
	Reverse: 5'- TGTCCAGATGTCGCGTCAG -3'		
G6PD (NG_009015)	Forward: 5'- AGACGAGCTGATGAAGAGAGTGG -3'	174	DNA
	Reverse: 5'- AATGTGCAGCTGAGGTCAATGG -3'		
GAPDH (NM_001256799.3)	Forward: 5'- AAATCAAGTGGGGCGATGCTG -3'	192	cDNA
	Reverse: 5'- TGATGATCTTGAGGCTGTTGTCA -3'		

95°C for 20 seconds, 58°C for 20 seconds, 72°C for 20 seconds, and post-denaturation for 3 minutes.

4. Results

4.1. All Protein-Coding Genes in the INK4-ARF Locus Are Homozygous Deleted in the A549 Cell Line

The presence of protein-coding genes located at the INK4-ARF locus at 9p21 region, including P15/*CDKN2B*-P16/*CDKN2A*-P14/*ARF*, was investigated at both DNA ([Figure 3A](#) and Appendices 9, 11, 13, 15 in Supplementary File contain the complete photographs of the gels) and *RNA* levels ([Figure 3B](#) and Appendices 10, 12, 14, 16 in Supplementary File contain the complete photographs of the gels) using specific primers. Based on our observations, the sequences of all three genes were lost in both investigated A549 cell lines. In the other examined cell lines used as control, including the normal diploid human lung cell line (MRC-5), the NSCLC cancer cell line (Calu-6), the liver carcinoma cell line (HepG2), and the sequences of all three protein-coding genes were detected at the DNA and m*RNA* levels.

4.2. ANRIL Long Non-coding RNA is Entirely Deleted in A549 Cells

To further investigate the presence of *ANRIL* in the 9p21 locus, 7 regions of the entire genomic sequence of this gene (126.3 kb) were examined, using specific primers ([Figure 4B](#)). In addition, the presence of several common exons of the *ANRIL* gene was also evaluated at the *RNA* level by conventional and real-time PCR. The conventional PCR products of all the genomic regions were observed on agarose gel electrophoresis for the MRC-5, Calu-6, and HepG2 cell lines. None of these targeted regions were amplified in the A549 cell line, confirming the absence of all these genomic regions in the investigated cells ([Figure 4A](#) and Appendices 1, 11, 2 - 6, 15 in Supplementary File contain the complete photographs of the gels). In contrast to other cell lines, none of the *ANRIL*'s targeted exons were amplified neither targeting DNA nor cDNA library indicating that this gene has no expression in the A549 cell line ([Figure

Figure 3. A, the amplification bands of the protein-coding genes (P14ARF, P15INK4B and P16INK4A) located at the ink4-ARF locus at the 9p21 region in the DNA extracted from the MRC-5, Calu-6, A549 and HepG2 cell lines; B, the amplification bands of the protein-coding genes (P14ARF, P15INK4B and P16INK4A) of the INK4-ARF locus at the 9p21 region in the cDNA libraries prepared from the MRC-5, Calu-6, A549 and HepG2 cell lines. NTC, non template control. See the Supplementary Figures section for the complete photography of the gels.

4C and Appendices 7, 8, 16 in Supplementary File contain the complete photographs of the gels). The level of *ANRIL* expression was also assessed by real-time PCR, where the data revealed no detectable *ANRIL RNA* for A549 cells, while *ANRIL* was expressed in the Calu-6 cell line. (Figure 5 and Appendix 17 in Supplementary File). All these results suggest that *ANRIL* is fully deleted in A549 cells.
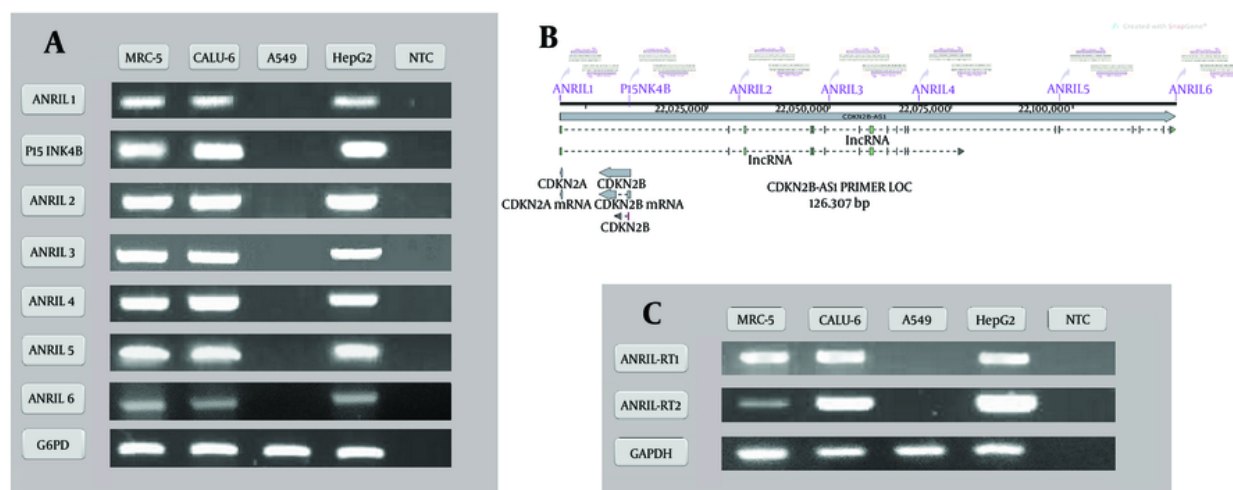
5. Discussion

Figure 4. A, the amplification bands of 7 different regions of the entire genomic sequence of lncRNA *ANRIL* in the DNA extracted from the MRC-5, Calu-6, A549 and HepG2 cell lines; B, the schematic map of seven selected genomic regions of the entire genomic sequence of lncRNA *ANRIL*; C, the amplification bands of the lncRNA *ANRIL* at the INK4-ARF locus in the cDNA libraries prepared from the MRC-5, Calu-6, A549 and HepG2 cell lines. NTC, non template control. See the Supplementary Figures section for the complete photography of the gels.

In this study, we examined the INK4-ARF locus in the 9p21 region by PCR at both DNA and *RNA* levels in the A549 cell line. We compared the results with normal human lung diploid cell lines (MRC-5), other non-small cell adenocarcinoma cell lines (Calu-6), and a cell line from a distinct cancer [human hepatocellular carcinoma (HepG2)]. Our analysis revealed that all protein-coding genes located at the INK4-ARF locus, including P15/*CDKN2B*, P16/*CDKN2A*, $P14^{ARF}$, as well as the long non-coding *RNA ANRIL* in the antisense of this locus, have fully deletion at the DNA level in the A549 cell line. Meanwhile, all of these genes are present and expressed in other cell lines that were investigated.

Since the presentation of the HeLa cell line in 1951, numerous cancer cell lines have been established and propagated, and they have been utilized in research regarding cancer biology and assessing the efficacy of anti-cancer agents, both *in-vitro* and as xenografts in laboratory animals (in vivo) (42).

The A549 cell line has been employed for over 5 decades as a model for type II alveolar cells, as well as an appropriate model for non-small cell lung adenocarcinoma in various studies (8).

Deletion of various encoding protein genes of the INK4-ARF locus at the 9p21 region, such as $P16^{INK4A}$ and $P15^{INK4B}$ has been reported in numerous cancers, including melanoma, glioma, lung cancer, and some leukemias, as well as cell lines linked to these cancers (43-45). In several studies, loss of heterozygosity at the 9p21 region was exhibited in 52% of NSCLC malignancies, while deletion of P16 was observed in 25% of NSCLC cases (46, 47). In a study conducted by Kraunz et al., a homozygous deletion of exon 2 of the P16 gene was reported in 34% of NSCLC samples, resulting in complete P16 protein deletion in more than half of these cases. According to their findings, this deletion is due to epigenetic silencing of 2 key genes involved in DNA double-strand break repair, the Fanconi anemia complementation group F (*FancF*) and Breast cancer type 1 susceptibility protein (BRCA1) genes (48). In another study, 58% of NSCLC tumors examined had an abnormality in the P16 gene, and homozygous deletion of this gene was reported in 48% of these cases (49). In the study by Panani et al., P16 gene deletion was identified in 8/11 squamous cell carcinoma, 5/6 adenocarcinoma, and 2/2 large cell lung cancer samples and this is a common finding in all subtypes of NSCLC (50). Homozygous deletion of $P16^{INK4A}$ is known to be one of the hallmarks of the A549 cell line (14, 35, 51, 52).

$P15^{INK4B}$ is an important protein that acts as a backup for P16 in cells. When P16 is lost, especially under stressful conditions, cells increase P15 protein levels to compensate for the loss (36). However, the simultaneous deletion of 2 *P15/Pl6* genes at the D9S126 locus (9p21) has been observed in tumors in NSCLC patients and cell
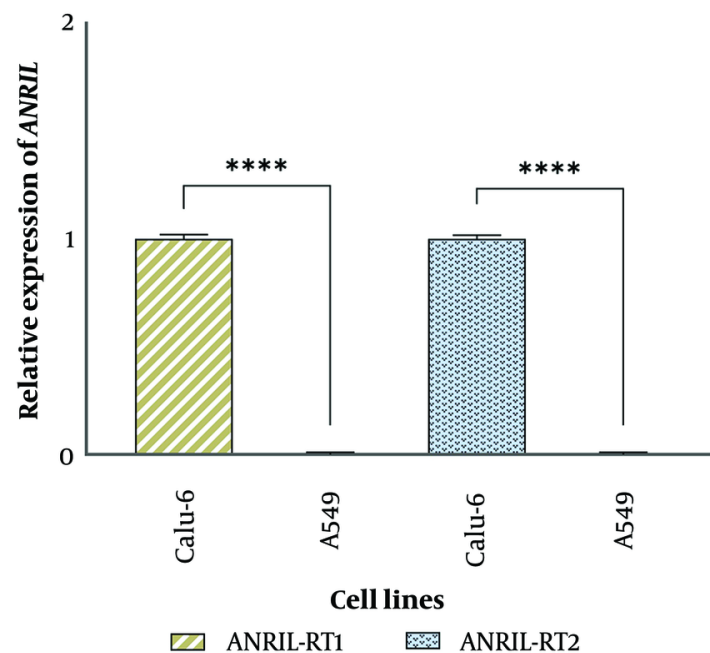
Figure 5. The real-time polymerase chain reaction (PCR) result of lncRNA *ANRIL* amplification for individual A549 and Calu-6 cell lines, showed the lack of expression of the *ANRIL* gene in A549 cells.

lines, including A549 cells ([37], [38], [53], [54]). *P14* ^{ARF} is another tumor suppressor gene co-located with P16 and *P15* at the INK4-ARF locus. Except for exon 1, the other 2 exons of this gene are similar in sequence to P16. *P14* ^{ARF} is deleted in 19% of NSCLC primary tumors and 25% of NSCLC cell lines, inter alia the A549 cell line ([7], [55]).

It has been previously reported that in more than 13% of NSCLC cell lines, including the A549 cell line, the *MTAP* gene is homozygously deleted. The *MTAP* gene is located on chromosome 9p21 ([34], [56], [57]) Interestingly, almost all (99%) of the tumors and various cell lines that had *MTAP* deletion also had *CDKN2A*/B loss ([58], [59]).

A bidirectional promoter in the 5' end of the *ANRIL* prime exon, flanking 300 bp upstream of the transcription initiation site of *P14* ^{ARF}, transcribed *ANRIL* in the antisense orientation of the INK4B-ARF- INK4-ARF gene cluster. Therefore, it would appear that the expression of the two genes is related to each other and is influenced by *E2F1* both in physiologic and pathologic conditions. It is interesting to note that the entire *P15*/*CDKN2B*-P16/*CDKN2A*-P14/ARF gene cluster and its transcriptional regulator gene (*ANRIL*) are part of 403 kb

germline deletion in the French family with melanoma, the family behind the discovery of *ANRIL* ([30], [60], [61]). Similarly, based on our observations, the entire INK4-ARF locus, including the protein-encoding genes P14, P15, P16, and the long non-coding *RNA ANRIL* were completely deleted in the A549 cells. The structural evidence indicates that the deletion of the long non-coding *RNA ANRIL* likely occurred concurrently with the deletion of other protein-coding genes within the INK4-ARF locus.

But how possible, that the search in databases and literature did not reveal any report regarding the lack of expression of the LncRNA *ANRIL* gene in the A549 cell line and there are several studies indicating the expression of *ANRIL* in this cell line?

Another hypothesis that could be responsible for the deletion of *ANRIL* in the A549 cell line is the inheritance of this deletion to a population derived from a single mutated cell.

Genomic instability is one of the hallmarks of cancers. Cancer cell lines have been propagated and immortalized from cancerous tissues for use in oncology research. Over time, during in vitro culture,

cancer cell lines may undergo genetic and phenotypic changes, leading to genetic heterogeneity and instability within a cell population (62).

A549 is an NSCLC cell line that homozygously expresses the endogenous KRAS G12S mutation (11, 12). A downstream effector protein in the RAS signaling pathway is the HMG box-containing protein 1 (*HBP1*) transcription factor. The *HBP1* enhances acetylation of the INK4A promoter by facilitating the activation of the histone acetyltransferase *P300* and *CREB* binding protein (CBP) (29). Boosting histone acetylation or inhibition of histone deacetylase activity, in turn, has been shown to induce incorrect kinetochore localization of mitotic checkpoint proteins and extend mitotic arrest (63). In addition to incorrect kinetochore localization, the extension of the mitotic process leads to increases in the possibility of errors in its various parts, such as the cell division machinery and the gene repair system, resulting in both numerical and structural chromosome abnormalities (62). It should be noted that the proximity to the common fragile region (FRA9G), the intranuclear architecture of chromatin, and the sensitivity of genomic segments of the *CDKN2A* locus as hotspots for DNA double-strand breaks and subsequent microhomology-mediated repair through non-homologous end joining (NHEJ) may be a major cause of homozygous deletion of INK4-ARF region (64-66). This mechanism may be a possible explanation for the occurrence of *ANRIL* deletion in the A549 cells.

5.1. Conclusions

Based on our observation, in addition to the protein-coding genes of the INK4ARF locus, including $P14^{ARF}$, $P16^{INK4A}$, and $P15^{INK4B}$ genes, the long non-coding *RNA ANRIL* is completely deleted in the A549 cell line.

Two scenarios can be considered to explain the deletion of LncRNA *ANRIL* in the A549 cell line. First, from a structural point of view, *ANRIL* shares a bidirectional promoter with the $P14^{ARF}$ gene and transcribes *ANRIL* in an antisense orientation to the INK4-ARF gene cluster. $P16^{INK4A}$ is located between *MTAP* and *ANRIL* in the vicinity of the first exon of *ANRIL*. $P15^{INK4B}$ is mapped to the inside of the first intron of *ANRIL* in antisense orientation. Given that various studies have reported that the *MTAP*, $P14^{ARF}$, $P16^{INK4A}$, and $P15^{INK4B}$ genes are deleted in the A549 cell line and that this deletion is one of the key characteristics of this cell line for use in related studies, it appears that *ANRIL* was also deleted at the time of the deletion of its antisense protein-coding genes. The second scenario

that could explain the deletion of *ANRIL* in the A549 cell line is the recent acquisition of this deletion in a population derived from a single mutated cell through successive passages under different conditions, notably considering that cancer cell lines, like cancer itself, are genetically unstable and always susceptible to acquiring new mutations.

Supplementary Material

Supplementary material(s) is available here [To read supplementary materials, please refer to the journal website and open PDF/HTML].

Footnotes

Authors' Contribution: Conceptualization: E. Sh., F. S., and Z. V.; Data curation: E. S., Z. V., and M. B. K. E.; Formal analysis: E. S., F. S., F. F., and K. R.; Funding acquisition: Z. V.; Investigation: E. S., F. S., and F. Z.; Methodology: Z. V., F. F., and M. B. K. E.; Project administration: Z. V. and F. F.; Resources: E.S., F.S., and F.Z.; Supervision: Z.V. and F. F.; Visualization: E. S. and F. Z.; Writing–original draft: E. S., F. Z., and F. F.; Writing–review and editing: Z. V. and K. R.

Conflict of Interests Statement: The authors declare that they have no conflict of interest for this paper.

Data Availability: The data presented in this study are uploaded during submission as a supplementary file and are openly available for readers upon request.

Ethical Approval: This study was approved by the Academic Research Ethics Committee of Kurdistan University of Medical Sciences with the ethics ID: IR.MUK.REC.1399.262 .

analysis, and interpretation of the data, writing of the report and the decision to submit the article for publication.

References

1. American Type Culture Collection organization. *Cell line collections organization and Detailed product information*. 2024. Available from: https://www.atcc.org/.

2. Foster KA, Oster CG, Mayer MM, Avery ML, Audus KL. Characterization of the A549 cell line as a type II pulmonary epithelial cell model for drug metabolism. *Exp Cell Res*. 1998;**243**(2):359-66. [PubMed ID: 9743595]. https://doi.org/10.1006/excr.1998.4172.

3. Cellosaurus. *The Cellosaurus, a cell line knowledge resource*. 2023. Available from: https://www.cellosaurus.org/.

4. Lieber M, Smith B, Szakal A, Nelson-Rees W, Todaro G. A continuous tumor-cell line from a human lung carcinoma with properties of type II alveolar epithelial cells. *Int J Cancer*. 1976;**17**(1):62-70. [PubMed ID: 175022]. https://doi.org/10.1002/ijc.2910170110.

5. Balis JU, Bumgarner SD, Paciga JE, Paterson JF, Shelley SA. Synthesis of lung surfactant-associated glycoproteins by A549 cells: description of an in vitro model for human type II cell dysfunction. *Exp Lung Res*. 1984;**6**(3-4):197-213. [PubMed ID: 6092046]. https://doi.org/10.3109/01902148409109248.

6. Garcia-de-Alba C. Repurposing A549 Adenocarcinoma Cells: New Options for Drug Discovery. *Am J Respir Cell Mol Biol*. 2021;**64**(4):405-6. [PubMed ID: 33596392]. [PubMed Central ID: PMC8008800]. https://doi.org/10.1165/rcmb.2021-0048ED.

7. Xie QC, Hu YD, Wang LL, Chen ZT, Diao XW, Wang ZX, et al. The co-transfection of p16(INK4a) and p14(ARF) genes into human lung cancer cell line A549 and the effects on cell growth and chemosensitivity. *Colloids Surf B Biointerfaces*. 2005;**46**(3):188-96. [PubMed ID: 16337111]. https://doi.org/10.1016/j.colsurfb.2005.10.006.

8. Korrodi-Gregorio L, Soto-Cerrato V, Vitorino R, Fardilha M, Perez-Tomas R. From Proteomic Analysis to Potential Therapeutic Targets: Functional Profile of Two Lung Cancer Cell Lines, A549 and SW900, Widely Studied in Pre-Clinical Research. *PLoS One*. 2016;**11**(11). e0165973. [PubMed ID: 27814385]. [PubMed Central ID: PMC5096714]. https://doi.org/10.1371/journal.pone.0165973.

9. Schabath MB, Cote ML. Cancer Progress and Priorities: Lung Cancer. *Cancer Epidemiol Biomarkers Prev*. 2019;**28**(10):1563-79. [PubMed ID: 31575553]. [PubMed Central ID: PMC6777859]. https://doi.org/10.1158/1055-9965.EPI-19-0221.

10. Blanco R, Iwakawa R, Tang M, Kohno T, Angulo B, Pio R, et al. A gene-alteration profile of human lung cancer cell lines. *Hum Mutat*. 2009;**30**(8):1199-206. [PubMed ID: 19472407]. [PubMed Central ID: PMC2900846]. https://doi.org/10.1002/humu.21028.

11. Werner AN, Kumar AI, Charest PG. CRISPR-mediated reversion of oncogenic KRAS mutation results in increased proliferation and reveals independent roles of Ras and mTORC2 in the migration of A549 lung cancer cells. *Mol Biol Cell*. 2023;**34**(13):ar128. [PubMed ID: 37729017]. [PubMed Central ID: PMC10848948]. https://doi.org/10.1091/mbc.E23-05-0152.

12. Desage AL, Leonce C, Swalduz A, Ortiz-Cuaran S. Targeting KRAS Mutant in Non-Small Cell Lung Cancer: Novel Insights Into Therapeutic Strategies. *Front Oncol*. 2022;**12**:796832. [PubMed ID: 35251972]. [PubMed Central ID: PMC8889932]. https://doi.org/10.3389/fonc.2022.796832.

13. Sitthideatphaiboon P, Galan-Cobo A, Negrao MV, Qu X, Poteete A, Zhang F, et al. STK11/LKB1 Mutations in NSCLC Are Associated with KEAP1/NRF2-Dependent Radiotherapy Resistance Targetable by Glutaminase Inhibition. *Clin Cancer Res*. 2021;**27**(6):1720-33. [PubMed

ID: 33323404]. [PubMed Central ID: PMC8138942]. https://doi.org/10.1158/1078-0432.CCR-20-2859.

14. Ikediobi ON, Davies H, Bignell G, Edkins S, Stevens C, O'Meara S, et al. Mutation analysis of 24 known cancer genes in the NCI-60 cell line set. *Mol Cancer Ther*. 2006;**5**(11):2606-12. [PubMed ID: 17088437]. [PubMed Central ID: PMC2705832]. https://doi.org/10.1158/1535-7163.MCT-06-0433.

15. Zhang W, Zhu J, Bai J, Jiang H, Liu F, Liu A, et al. Comparison of the inhibitory effects of three transcriptional variants of CDKN2A in human lung cancer cell line A549. *J Exp Clin Cancer Res*. 2010;**29**(1):74. [PubMed ID: 20565749]. [PubMed Central ID: PMC2897778]. https://doi.org/10.1186/1756-9966-29-74.

16. Aoyama Y, Avruch J, Zhang XF. Nore1 inhibits tumor cell growth independent of Ras or the MST1/2 kinases. *Oncogene*. 2004;**23**(19):3426-33. [PubMed ID: 15007383]. https://doi.org/10.1038/sj.onc.1207486.

17. Donninger H, Calvisi DF, Barnoud T, Clark J, Schmidt ML, Vos MD, et al. NORE1A is a Ras senescence effector that controls the apoptotic/senescent balance of p53 via HIPK2. *J Cell Biol*. 2015;**208**(6):777-89. [PubMed ID: 25778922]. [PubMed Central ID: PMC4362463]. https://doi.org/10.1083/jcb.201408087.

18. Breuer RH, Postmus PE, Smit EF. Molecular pathology of non-small-cell lung cancer. *Respiration*. 2005;**72**(3):313-30. [PubMed ID: 15942304]. https://doi.org/10.1159/000085376.

19. Kobayashi S, Shimamura T, Monti S, Steidl U, Hetherington CJ, Lowell AM, et al. Transcriptional profiling identifies cyclin D1 as a critical downstream effector of mutant epidermal growth factor receptor signaling. *Cancer Res*. 2006;**66**(23):11389-98. [PubMed ID: 17145885]. https://doi.org/10.1158/0008-5472.CAN-06-2318.

20. Rouillard AD, Gundersen GW, Fernandez NF, Wang Z, Monteiro CD, McDermott MG, et al. The harmonizome: a collection of processed datasets gathered to serve and mine knowledge about genes and proteins. *Database (Oxford)*. 2016;**2016**. [PubMed ID: 27374120]. [PubMed Central ID: PMC4930834]. https://doi.org/10.1093/database/baw100.

21. Shapiro GI, Koestner DA, Matranga CB, Rollins BJ. Flavopiridol induces cell cycle arrest and p53-independent apoptosis in non-small cell lung cancer cell lines. *Clin Cancer Res*. 1999;**5**(10):2925-38. [PubMed ID: 10537362].

22. Fukazawa T, Maeda Y, Matsuoka J, Yamatsuji T, Shigemitsu K, Morita I, et al. Inhibition of Myc effectively targets KRAS mutation-positive lung cancer expressing high levels of Myc. *Anticancer Res*. 2010;**30**(10):4193-200. [PubMed ID: 21036740].

23. Shen H, Dong W, Gao D, Wang G, Ma G, Liu Q, et al. MDM2 antagonist Nutlin-3a protects wild-type p53 cancer cells from paclitaxel. *Chinese Science Bulletin*. 2012;**57**(9):1007-12. https://doi.org/10.1007/s11434-012-4984-7.

24. Gerullis D, Rensing L, Beyersmann D. Heat shock treatment decreases E2F1-DNA binding and E2F1 levels in human A549 cells. *Biol Chem*. 2003;**384**(1):161-7. [PubMed ID: 12674510]. https://doi.org/10.1515/BC.2003.017.

25. Feng DD, Cao Q, Zhang DQ, Wu XL, Yang CX, Chen YF, et al. Transcription factor E2F1 positively regulates interferon regulatory factor 5 expression in non-small cell lung cancer. *Onco Targets Ther*. 2019;**12**:6907-15. [PubMed ID: 31692554]. [PubMed Central ID: PMC6711570]. https://doi.org/10.2147/OTT.S215701.

26. Wu A, Wu B, Guo J, Luo W, Wu D, Yang H, et al. Elevated expression of CDK4 in lung cancer. *J Transl Med*. 2011;**9**:38. [PubMed ID: 21477379]. [PubMed Central ID: PMC3094221]. https://doi.org/10.1186/1479-5876-9-38.

27. Zhang XH, Cheng Y, Shin JY, Kim JO, Oh JE, Kang JH. A CDK4/6 inhibitor enhances cytotoxicity of paclitaxel in lung adenocarcinoma cells harboring mutant KRAS as well as wild-type

KRAS. *Cancer Biol Ther*. 2013;**14**(7):597-605. [PubMed ID: 23792647]. [PubMed Central ID: PMC3742489]. https://doi.org/10.4161/cbt.24592.

28. Kong Y, Hsieh CH, Alonso LC. ANRIL: A lncRNA at the CDKN2A/B Locus With Roles in Cancer and Metabolic Disease. *Front Endocrinol (Lausanne)*. 2018;**9**:405. [PubMed ID: 30087655]. [PubMed Central ID: PMC6066557]. https://doi.org/10.3389/fendo.2018.00405.

29. Farooq U, Notani D. Transcriptional regulation of INK4/ARF locus by cis and trans mechanisms. *Front Cell Dev Biol*. 2022;**10**:948351. [PubMed ID: 36158211]. [PubMed Central ID: PMC9500187]. https://doi.org/10.3389/fcell.2022.948351.

30. Lee AM, Ferdjallah A, Moore E, Kim DC, Nath A, Greengard E, et al. Long Non-Coding RNA ANRIL as a Potential Biomarker of Chemosensitivity and Clinical Outcomes in Osteosarcoma. *Int J Mol Sci*. 2021;**22**(20). [PubMed ID: 34681828]. [PubMed Central ID: PMC8538287]. https://doi.org/10.3390/ijms222011168.

31. Congrains A, Kamide K, Ohishi M, Rakugi H. ANRIL: molecular mechanisms and implications in human health. *Int J Mol Sci*. 2013;**14**(1):1278-92. [PubMed ID: 23306151]. [PubMed Central ID: PMC3565320]. https://doi.org/10.3390/ijms14011278.

32. Zhang EB, Kong R, Yin DD, You LH, Sun M, Han L, et al. Long noncoding RNA ANRIL indicates a poor prognosis of gastric cancer and promotes tumor growth by epigenetically silencing of miR-99a/miR-449a. *Oncotarget*. 2014;**5**(8):2276-92. [PubMed ID: 24810364]. [PubMed Central ID: PMC4039162]. https://doi.org/10.18632/oncotarget.1902.

33. Lou N, Liu G, Pan Y. Long noncoding RNA ANRIL as a novel biomarker in human cancer. *Future Oncol*. 2020;**16**(35):2981-95. [PubMed ID: 32986472]. https://doi.org/10.2217/fon-2020-0470.

34. Hori H, Tran P, Carrera CJ, Hori Y, Rosenbach MD, Carson DA, et al. Methylthioadenosine phosphorylase cDNA transfection alters sensitivity to depletion of purine and methionine in A549 lung cancer cells. *Cancer Res*. 1996;**56**(24):5653-8. [PubMed ID: 8971171].

35. Bai XY, Che FX, Chen XM, Meng LY, Zhou Y. p16INK4a expression mediated by recombinant adenovirus can induce senescence of A549 cells. *Chin J Experiment Clin Virol*. 2004;**18**(1):54-8.

36. Camacho CV, Mukherjee B, McEllin B, Ding LH, Hu B, Habib AA, et al. Loss of p15/Ink4b accompanies tumorigenesis triggered by complex DNA double-strand breaks. *Carcinogenesis*. 2010;**31**(10):1889-96. [PubMed ID: 20663777]. [PubMed Central ID: PMC2950935]. https://doi.org/10.1093/carcin/bgq153.

37. Hu Y, Liao M, Ding J, Zhou J, Xu K. Co-deletion of both p15/p16 genes correlates with poor prognosis non-small cell lung cnacer. *Chin J Cancer Res*. 2002;**14**(3):216-9. https://doi.org/10.1007/s11670-002-0048-x.

38. Yoshizaki K, Katakura Y, Fujiki T, Tsunematu T, Teruya K, Shirahata S. Hydrogen Peroxide-Induced Cellular Senescence is Regulated via Two Different Pathways. In: Gòdia F, Fussenegger M, editors. *Animal Cell Technology Meets Genomics: Proceedings of the 18th ESACT Meeting Granada, Spain, May 11-14, 2003*. New York, USA: Springer; 2005.

39. Xu R, Mao Y, Chen K, He W, Shi W, Han Y. The long noncoding RNA ANRIL acts as an oncogene and contributes to paclitaxel resistance of lung adenocarcinoma A549 cells. *Oncotarget*. 2017;**8**(24):39177-84. [PubMed ID: 28402932]. [PubMed Central ID: PMC5503604]. https://doi.org/10.18632/oncotarget.16640.

40. Lin L, Gu ZT, Chen WH, Cao KJ. Increased expression of the long non-coding RNA ANRIL promotes lung cancer cell metastasis and correlates with poor prognosis. *Diagn Pathol*. 2015;**10**:14. [PubMed ID: 25889788]. [PubMed Central ID: PMC4599723]. https://doi.org/10.1186/s13000-015-0247-7.

41. Wang X, Zhang G, Cheng Z, Dai L, Jia L, Jing X, et al. Knockdown of lncRNA ANRIL inhibits the development of cisplatin resistance by upregulating miR-98 in lung cancer cells. *Oncol Rep*. 2020;**44**(3):1025-36. [PubMed ID: 32705261]. https://doi.org/10.3892/or.2020.7685.

42. Gillet JP, Varma S, Gottesman MM. The clinical relevance of cancer cell lines. *J Natl Cancer Inst*. 2013;**105**(7):452-8. [PubMed ID: 23434901]. [PubMed Central ID: PMC3691946]. https://doi.org/10.1093/jnci/djt007.

43. Hirama T, Koeffler HP. Role of the cyclin-dependent kinase inhibitors in the development of cancer. *Blood*. 1995;**86**(3):841-54. [PubMed ID: 7620180].

44. Kamb A, Gruis NA, Weaver-Feldhaus J, Liu Q, Harshman K, Tavtigian SV, et al. A cell cycle regulator potentially involved in genesis of many tumor types. *Sci*. 1994;**264**(5157):436-40. [PubMed ID: 8153634]. https://doi.org/10.1126/science.8153634.

45. Fujita M, Enomoto T, Haba T, Nakashima R, Sasaki M, Yoshino K, et al. Alteration ofp16 andp15 genes in common epithelial ovarian tumors. *Int J Cancer*. 1997;**74**(2):148-55. https://doi.org/10.1002/(sici)1097-0215(19970422)74:2<148::Aid-ijc2>3.0.Co;2-z.

46. Packenham JP, Taylor JA, White CM, Anna CH, Barrett JC. Homozygous deletions at chromosome 9p21 and mutation analysis of p16 and p15 in microdissected primary non-small cell lung cancers. *Lung Cancer*. 1995;**13**(3):327-8. https://doi.org/10.1016/0169-5002(96)84238-3.

47. Nakagawa K, Conrad NK, Williams JP, Johnson BE, Kelley MJ. Mechanism of inactivation of CDKN2 and MTS2 in non-small cell lung cancer and association with advanced stage. *Oncogene*. 1995;**11**(9):1843-51. [PubMed ID: 7478613].

48. Kraunz KS, Nelson HH, Lemos M, Godleski JJ, Wiencke JK, Kelsey KT. Homozygous deletion of p16INK4a and tobacco carcinogen exposure in nonsmall cell lung cancer. *Int J Cancer*. 2006;**118**(6):1364-9. [PubMed ID: 16184554]. https://doi.org/10.1002/ijc.21522.

49. Gazzeri S, Gouyer V, Vour'ch C, Brambilla C, Brambilla E. Mechanisms of p16INK4A inactivation in non small-cell lung cancers. *Oncogene*. 1998;**16**(4):497-504. [PubMed ID: 9484839]. https://doi.org/10.1038/sj.onc.1201559.

50. Panani AD, Maliaga K, Babanaraki A, Bellenis I. Numerical abnormalities of chromosome 9 and p16CDKN2A gene deletion detected by FISH in non-small cell lung cancer. *Anticancer Res*. 2009;**29**(11):4483-7. [PubMed ID: 20032395].

51. Tian Y, Zhou J, Qiao J, Liu Z, Gu L, Zhang B, et al. Detection of somatic copy number deletion of the CDKN2A gene by quantitative multiplex PCR for clinical practice. *Front Oncol*. 2022;**12**:1038380. [PubMed ID: 36531022]. [PubMed Central ID: PMC9755846]. https://doi.org/10.3389/fonc.2022.1038380.

52. Ichikawa M, Muramatsu N, Matsunaga W, Ishikawa T, Okuda T, Okamoto H, et al. Effects of inhalable gene transfection as a novel gene therapy for non-small cell lung cancer and malignant pleural mesothelioma. *Sci Rep*. 2022;**12**(1):8634. [PubMed ID: 35606391]. [PubMed Central ID: PMC9126906]. https://doi.org/10.1038/s41598-022-12624-4.

53. Shan Z, Parker T, Wiest JS. Identifying novel homozygous deletions by microsatellite analysis and characterization of tumor suppressor candidate 1 gene, TUSC1, on chromosome 9p in human lung cancer. *Oncogene*. 2004;**23**(39):6612-20. [PubMed ID: 15208665]. [PubMed Central ID: PMC3449089]. https://doi.org/10.1038/sj.onc.1207857.

54. Fountain JW, Hudson TJ, Engelstein M, Housman DE, Dracopoli NC. Dinucleotide repeat polymorphism at the D9S126 locus (9p21). *Hum Mol Genet*. 1993;**2**(6):823. [PubMed ID: 8353508]. https://doi.org/10.1093/hmg/2.6.823-a.

55. Nicholson SA, Okby NT, Khan MA, Welsh JA, McMenamin MG, Travis WD, et al. Alterations of p14ARF, p53, and p73 genes involved in the E2F-1-mediated apoptotic pathways in non-small cell lung carcinoma. *Cancer Res*. 2001;**61**(14):5636-43. [PubMed ID: 11454718].

56. Ashok Kumar P, Graziano SL, Danziger N, Pavlick D, Severson EA, Ramkissoon SH, et al. Genomic landscape of non-small-cell lung cancer with methylthioadenosine phosphorylase (MTAP) deficiency.

Cancer Med. 2023;**12**(2):1157-66. [PubMed ID: 35747993]. [PubMed Central ID: PMC9883541]. https://doi.org/10.1002/cam4.4971.

57. Menezes WP, Silva VAO, Gomes INF, Rosa MN, Spina MLC, Carloni AC, et al. Loss of 5'-Methylthioadenosine Phosphorylase (MTAP) is Frequent in High-Grade Gliomas; Nevertheless, it is Not Associated with Higher Tumor Aggressiveness. *Cells.* 2020;**9**(2). [PubMed ID: 32093414]. [PubMed Central ID: PMC7072758]. https://doi.org/10.3390/cells9020492.

58. Mauri G, Patelli G, Roazzi L, Amatu A, Calvanese G, Martinelli F, et al. 112P Clinicopathological characterization of MTAP-altered metastatic gastrointestinal tumors. *Ann Oncol.* 2022;**33**. https://doi.org/10.1016/j.annonc.2022.09.113.

59. Alhalabi O, Chen J, Zhang Y, Lu Y, Wang Q, Ramachandran S, et al. MTAP deficiency creates an exploitable target for antifolate therapy in 9p21-loss cancers. *Nat Commun.* 2022;**13**(1):1797. [PubMed ID: 35379845]. [PubMed Central ID: PMC8980015]. https://doi.org/10.1038/s41467-022-29397-z.

60. Pasmant E, Laurendeau I, Heron D, Vidaud M, Vidaud D, Bieche I. Characterization of a germ-line deletion, including the entire INK4/ARF locus, in a melanoma-neural system tumor family: identification of ANRIL, an antisense noncoding RNA whose expression coclusters with ARF. *Cancer Res.* 2007;**67**(8):3963-9. [PubMed ID: 17440112]. https://doi.org/10.1158/0008-5472.CAN-06-2004.

61. Aguilo F, Di Cecilia S, Walsh MJ. Long Non-coding RNA ANRIL and Polycomb in Human Cancers and Cardiovascular Disease. *Curr Top*

Microbiol Immunol. 2016;**394**:29-39. [PubMed ID: 26220772]. [PubMed Central ID: PMC4732918]. https://doi.org/10.1007/82_2015_455.

62. He Z, Wilson A, Rich F, Kenwright D, Stevens A, Low YS, et al. Chromosomal instability and its effect on cell lines. *Cancer Rep (Hoboken).* 2023;**6**(6). e1822. [PubMed ID: 37095005]. [PubMed Central ID: PMC10242654]. https://doi.org/10.1002/cnr2.1822.

63. Shin HJ, Baek KH, Jeon AH, Kim SJ, Jang KL, Sung YC, et al. Inhibition of histone deacetylase activity increases chromosomal instability by the aberrant regulation of mitotic checkpoint activation. *Oncogene.* 2003;**22**(25):3853-8. [PubMed ID: 12813458]. https://doi.org/10.1038/sj.onc.1206502.

64. Kohno T, Yokota J. Molecular processes of chromosome 9p21 deletions causing inactivation of the p16 tumor suppressor gene in human cancer: deduction from structural analysis of breakpoints for deletions. *DNA Repair (Amst).* 2006;**5**(9-10):1273-81. [PubMed ID: 16931177]. https://doi.org/10.1016/j.dnarep.2006.05.021.

65. Bignell GR, Greenman CD, Davies H, Butler AP, Edkins S, Andrews JM, et al. Signatures of mutation and selection in the cancer genome. *Nature.* 2010;**463**(7283):893-8. [PubMed ID: 20164919]. [PubMed Central ID: PMC3145113]. https://doi.org/10.1038/nature08768.

66. Sawinska M, Schmitt JG, Sagulenko E, Westermann F, Schwab M, Savelyeva L. Novel aphidicolin-inducible common fragile site FRA9G maps to 9p22.2, within the C9orf39 gene. *Genes Chromosomes Cancer.* 2007;**46**(11):991-9. [PubMed ID: 17668870]. https://doi.org/10.1002/gcc.20484.